Ethiopian Journal of Science and Sustainable Development

e-ISSN 2663-3205 *Volume 13 (1), 2026*

Journal Home Page: www.ejssd.astu.edu.et

Research Paper

Quantification and Evaluation of Radon-222 in Groundwater of Flood-Affected Areas in Borno State, North-Eastern Nigeria: Implications for Lung Cancer Risk

Aliyu Adamu[1*], Muhammad Hassan[1,2], Salamatu S. Jere[2], Musa H. Umar[1]

[1]*Department of Physics, University of Maiduguri, Maiduguri, Nigeria*
[2]*Centre for Nuclear Energy Research and Training, University of Maiduguri, Maiduguri, Nigeria*

Article Info

Article History:
Received 21 June 2025
Received in revised form 17 August 2025
Accepted 21 August 2025

Keywords:
age,
alpha radiation,
flood-prone areas,
internal organs,
sex

Abstract

Radon-222 (^{222}Rn), a naturally occurring radioactive gas, which is soluble in water may damage internal organs if ingested or inhaled. This study investigated the concentration of ^{222}Rn in groundwater of 28 locations across five flood-affected areas of Borno state, in September 2024. Groundwater samples were collected and analyzed using a Tri-Carb-LSA 1000 Liquid Scintillation Counter. Elevated levels of ^{222}Rn were recorded in Jere (12.35 Bq/L), Konduga (11.33 Bq/L), and Magumeri (10.81 Bq/L). The concentrations in Konduga and Jere exceed the U.S. Environmental Protection Agency maximum contaminant level of 11.1 Bq/L. The total (ingestion and inhalation) annual effective doses varied by age and sex and ranged between 6.57 and 69.49 µSv/y for males, and between 2.01 and 64.52 µSv/y for females. Stomach received the highest absorbed doses (4.83–57.20 µSv/y), consistent with its role as the primary reservoir for ingested water. Lungs also received non-negligible doses of up to 12.11 µSv/y through systemic circulation. Over 95% of the total internal organ dose was attributable to alpha radiation, known for its high linear energy transfer and potential to cause cellular damage. This underscores a significant risk of gastrointestinal cancers and compounds the lung cancer risk. Adults had higher dose burdens than children due to larger water intake volumes. Males exhibited slightly elevated organ doses compared to females, likely due to physiological and metabolic differences. The findings emphasize the need for targeted public health interventions, including regular radon monitoring, awareness creation, and the introduction of point-of-use water treatment systems to mitigate exposure.

1. Introduction

Radon-222 is a naturally occurring radioactive noble gas and a concerning environmental contaminant that poses significant public health risks worldwide (Janik, 2022; Akinnagbe et al., 2018; Amin et al., 2017; Ali et al., 2010). Originating from the radioactive decay of uranium (^{238}U) present in rocks, water, and air, radon is a colorless, odorless, and chemically inert gas (Kumar et al., 2022; UNSCEAR, 1988), rendering it undetectable by human senses alone. Despite its inert nature, radon's radioactive properties and its ability to accumulate in enclosed spaces make it an environmental hazard of concern (Elola et al., 2023).

Distinguished as the heaviest among noble gases, radon exhibits unique physical properties, including the highest melting point, boiling point, critical temperature, and critical pressure (Kumar et al., 2022; UNSCEAR, 2008). This gas is naturally present in most materials and is particularly emitted through rocks and construction materials situated on the ground surface. Comprising a substantial portion (approximately 54%

*Corresponding author, e-mail: Aliyuphysics@unimaid.edu.ng

https://doi.org/10.20372/ejssdastu:v13.i1.2026.1012

(Sextro, 1994)) of the natural background radiation exposure experienced by living organisms, radon-222 stands as a major contributor to the overall radiation dose received by the human population (Amin et al., 2017; Ali et al., 2010; Manzoor et al.,2008; UNSCEAR, 2008).

Among the known isotopes of radon (Aruwa et al., 2017; Deveci & Oncel, 2023), radon-222 is the most significant, with a half-life of 3.82 *days* (Kumar et al., 2022; Garba et al., 2012). This radioactive gas is produced during the decay of uranium-238 (^{238}U) in the Earth's crust (Janik, 2022). It undergoes radioactive decay, emitting alpha particles and transforming into a series of electrically charged atoms known as radon progeny (Ali et al., 2010). The progenies include polonium-218 (^{218}Po) and lead-214 (^{214}Pb) (Mostafa et al., 2022). The transformation underscores the radiological importance of radon, influencing its environmental behavior and health risks. Radon-222 is produced continuously through the decay of radium (^{226}Ra) and emits alpha particles during its transformation.

Radon's tendency to accumulate in confined spaces, such as residential areas, stems from its physical properties and mode of formation (Elola et al., 2023; Kumar et al., 2022; Ajibola et al., 2021). Being denser than air (Ali et al., 2010), radon tends to concentrate in poorly ventilated areas, particularly indoors (Kumar et al., 2022; Wilkening, 1990). Once released, radon decays into its progeny (Mostafa et al., 2022), which can attach to indoor airborne particles like dust (Binesh et al., 2010; Wilkening, 1990). As a noble gas, radon is chemically inert, allowing it to move freely through rocks, groundwater, and air (Olise et al., 2016). Kumar et al. (2022) noted that this characteristic, along with its colorless and odorless nature, poses a significant health risk. The ability of radon to migrate through the Earth's crust and groundwater, coupled with its potential for indoor accumulation, underscores the importance of understanding its environmental dynamics and transport pathways (Darabi et al., 2020; Cho et al., 2004).

The alpha particles emitted during the decay of radon, with energies ranging from 5.49 to 7.69 *MeV*, can induce significant DNA damage, particularly in lung tissue. When inhaled, these particles may settle on the mucosal lining of the respiratory tract, initiating a series of radiological and biological processes that can lead to lung cancer (Binesh et al., 2010; Amin et al., 2015). In fact, radon is recognized as the second leading cause of lung cancer, after smoking (Umar et al., 2024; Ajibola et al., 2021), and is responsible for a significant proportion of lung cancer cases worldwide (Elola et al., 2023). This risk is higher among smokers due to the synergistic effects of tobacco and radon exposure (Lorenzo-Gonzalez et al., 2020).

Beyond inhalation, radon exposure can also occur through ingestion of contaminated water, which may lead to stomach cancer (Mostafa et al., 2022; Akinnagbe et al., 2018; Aruwa et al., 2017; Binesh et al., 2010; Duggal et al., 2012; Nikolopoulos & Louizi, 2008). While the health risks associated with radon ingestion are generally considered lower than those from inhalation, the presence of radon in drinking water remains a concern, particularly in regions where groundwater is primary source of drinking (Kumar et al., 2022; Mostafa et al., 2022; Ajibola et al., 2021; El-Arabya et al., 2019; Akinnagbe et al., 2018). Thus, the association of radon exposure with lung and stomach cancers makes it critical to assess its concentration in drinking water, particularly in areas affected by flooding (Umar et al., 2024). In its nature, radon is soluble in water (Kumar et al., 2022; UNSCEAR, 1988); hence, when the water is used, radon gas can be released into the air, contributing to indoor radon concentrations and potentially increasing inhalation exposure (Kumar et al., 2022; Ali et al., 2010).

Effective strategies for managing radon exposure involve a combination of monitoring, mitigation, and public education efforts (Ajibola et al., 2021; Bello et al., 2020; Ali et al., 2010; UNSCEAR, 2008; USEPA, 1991). Recent studies emphasize the importance of monitoring radon concentrations and evaluating their impact on public health (Celen et al., 2023; Elola et al., 2023). Mitigation techniques, such as sealing cracks in foundations, improving ventilation, and installing radon reduction systems, can significantly reduce radon concentrations in indoor environments (Ali et al., 2010; Nikolopoulos & Louizi, 2008; WHO, 2004). Given the significant health risks associated with radon exposure, particularly lung cancer, ongoing research is essential for gaining a deeper understanding of radon's environmental behavior, health effects, and effective

management strategies (Celen et al., 2023; Nakale et al., 2023; Darby et al., 2005; UNSCEAR, 1988, 2008). Thus, by elucidating the complex interactions among radon, the environment, and human health, this study tried to inform policy makers and experts to target minimizing its exposure to cancer and hence to safeguard public health.

2. Materials and Methods

2.1 Study area

With a surface of roughly 70,898 km^2, Borno State is the largest in Nigeria. It is situated in the northeastern part of the country at Latitude of 11.85°N, and Longtude of 13.08°E. It has borders with the Nigerian states of Yobe, Gombe, and Adamawa as well as Niger to the northwest, Chad to the north, and Cameroon to the east. The political and economic center is Maiduguri, the country's capital. The state is located in the Sudano-Sahelian climate zone, which is distinguished by a brief rainy season (June-Sep.) with annual rainfall ranging from roughly 300 mm in the north to 800 mm in the south, and a lengthy dry season (October–May) that is dominated by the dusty Harmattan winds. While the Harmattan can reduce night-time temperatures to about 15 °C, year-round temperatures are typically high, averaging 25 to 32 °C, but frequently going beyond 40 °C during the hottest dry months. With the exception of the rainy season, the humidity is low for the majority of the year. The study area includes flood-prone Local Government Areas (LGAs), namely Jere, Konduga, Mafa, and Magumeri, where September flooding impacts water quality and increases the risk of contamination from naturally occurring radionuclides.

Intense rainfall events, such as those observed in September 2023, have led to severe flooding in Maiduguri, Jere, and Konduga, displacing residents and contributing to the leaching of naturally occurring radionuclides into water sources, posing a significant risk to public health.

2.2 Sample collection and preparation

Random sampling was employed to ensure unbiased representation of water sources within the study area. One liter plastic containers were used to collect samples from twenty-eight groundwater sources. Prior to collection, the containers were thoroughly washed and rinsed with distilled water to minimize contamination. Borehole water was evacuated for a few minutes before collection, and well water was purged. To prevent carbon dioxide trapping and to preserve sample integrity, the containers were filled to the brim and immediately acidified with nitric acid. The samples were transported to the Scintillation Laboratory at the Centre for Energy Research and Training, A.B.U. Zaria, within 48 h. Sample preparation involved adding 10 mL of each water sample to 10 ml of liquid scintillation solution in airtight vials. The vials were vigorously shaken for three minutes to facilitate ^{222}Rn extraction into the organic scintillant. Samples were then allowed to equilibrate for a minimum of three hours before counting.

2.3 Concentration of ^{222}Rn in groundwater

The concentration of ^{222}Rn in the sample at the time of collection was determined using the equation (Bello et al., 2025),

$$C_{Rn}(Bq\ L^{-1}) = \frac{100\cdot(T_c - B_c)\cdot e^{\lambda t}}{60\cdot f\cdot \gamma_c} \qquad (1)$$

where C_{Rn} is the ^{222}Rn concentration at sampling time, Tc is the sample total count rate (counts min^{-1}), B_c is the background count rate (counts min^{-1}), t = 4320 min (72 h) is the elapsed time between sample collection and counting (min), f = 13.47 is the calibration factor, γ_c = 0.964 is the fraction of ^{222}Rn in the cocktail and

$$\lambda = \frac{\ln 2}{T_{1/2}} = 1.76 \times 10^{-4}\ min^{-1}$$

is the ^{222}Rn decay constant.

2.4 Dose estimation

Radon dissolved in household water poses a dual exposure risk through ingestion and inhalation. Radon present in drinking water poses a significant health risk due to its ingestion and subsequent deposition in stomach tissues, which can contribute to gastrointestinal cancers. The cancer risk arising from ingested radon is derived from calculations of the absorbed dose in the stomach tissues, with studies estimating that approximately 30% of radon activity concentration remains integrated in the stomach lining (UNSCEAR, 2008).

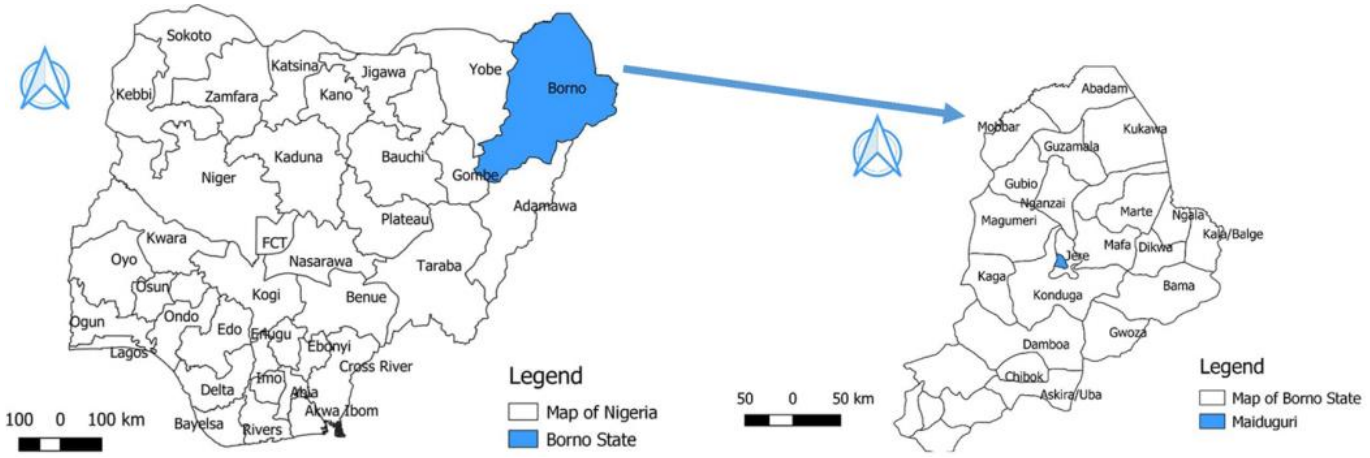

Figure 1: Map of Nigeria indicating Borno State and Map of Borno State showing Maiduguri (blue), Jere, Konduga, Mafa, and Magumeri, the study areas (Source: Kwaghe et al., 2023)

2.4.1 Ingested waterborne radon mean effective dose

The Annual Effective Dose from ingestion, δ_{ing} was determined using (UNSCEAR, 2008),

$$\delta_{\text{ing}}(\mu Sv/y) = C_{Rn} \cdot \varsigma_i^{\text{ing}} \cdot d_{wi} \cdot T \qquad (2)$$

Where C_{Rn} is the mean ^{222}Rn activity concentration in water, d_{wi} is the daily water ingestion, ς_i^{ing} is the ingestion dose conversion factor ($Sv \cdot Bq^{-1}$), given in Table 1 (ICRP, 1993; Howard et al., 2020), T is the exposure duration ($365\ d \cdot y^{-1}$).

2.4.2 Inhaled waterborne radon mean effective dose

Inhalation of radon released from domestic water during activities such as cooking, bathing, and laundering is also a potential health hazard. The World Health Organization (WHO, 2011) estimates that 1–7% of all lung cancer deaths globally are attributable to elevated radon levels in water. Furthermore, 10–15% of total indoor radon can result from the outgassing of radon from tap water. The annual effective inhalation dose from breathing in radon released from water is estimated using the following equation (UNSCEAR, 2008; ICRP, 1993),

$$\delta_{\text{inh}}(\mu Sv\ y^{-1}) = C_{Rn} \cdot \gamma_{aw} \cdot \varsigma_i^{\text{inh}} \cdot \gamma \cdot \varepsilon \qquad (3)$$

where γ_{aw} is the ratio of ^{222}Rn in air to water (typically 10^{-4}), ς_i^{inh} is the dose conversion factor (Table 1), $\gamma = 7000\ h \cdot y^{-1}$ is the annual indoor exposure duration and ε is the indoor equilibrium factor between radon and its progeny (global average $\varepsilon = 0.4$).

Table 1: Age-dependent inhalation coefficients, μ_{inh} and ingestion coefficients, μ_{ing} by life stage and sex (ICRP, 1993; Howard et al., 2020)

i	Life stage	$\varsigma_i^{\text{inh}}(nSv \cdot h^{-1} \cdot (Bq \cdot m^{-3})^{-1})$	$\varsigma_i^{\text{ing}}(10^{-8}\ Sv \cdot\ Bq^{-1})$	$D_i\ (L \cdot day^{-1})$	
				Male	Female
1	0–6 months	8.4	3.2	0.7	0.7
2	7–12 months	5.6	2.1	0.8	0.8
3	1–3 years	4.1	1.4	1.3	1.3
4	4–8 years	3.4	1.1	1.7	1.7
5	9–13 years	3.4	1.1	2.4	2.1
6	14–18 years	3.4	1.1	3.3	2.3
7	>19 years	3.0	1.0	3.7	2.7
8	Pregnancy	3.0	1.0	NA	3.0
9	Lactation	3.0	1.0	NA	3.8

Note: NA indicates data not applicable

Then, the total annual effective dose from both ingestion and inhalation was computed as,

$$\delta_{\text{total}} = \delta_{\text{ing}} + \delta_{\text{inh}} \quad (4)$$

2.5 Dose estimation and risk assessment models

The decay chain of ^{222}Rn involves high-linear energy transfer (LET) radiation, primarily through alpha emissions, and proceeds as follows: ^{222}Rn (α: 5.77 *MeV*, $t_{1/2}$ = 3.82 *days*) decays to ^{218}Po (α: 2.37 *MeV*, $t_{1/2}$ = 3.10 *min*), then to ^{214}Pb (β^-: 2.55 *MeV*, $t_{1/2}$ = 26.8 *min*), followed by ^{214}Bi (β^-: 3.48 *MeV*, $t_{1/2}$ = 19.9 *min*), then ^{214}Po (α: -3.79 *MeV*, $t_{1/2}$=164 μs), and finally ^{210}Pb ($t_{1/2}$ = 22.3 *years*) before reaching stable lead. The alpha particles, especially from ^{218}Po and ^{214}Po, have a high relative biological effectiveness (RBE ≈ 20) due to their dense ionization, causing significant biological injury when inhaled and deposited in the bronchial epithelium (Fan e al., 2023; Sridhar et al., 2021; Eikenberg, 2002).

2.5.1 Organ-specific annual effective dose

The annual effective dose for the lungs, δ_{lung} is calculated using the equation (UNSCEAR, 2000),

$$\delta_{\text{lung}}(\mu Sv^{-1}) = \delta_{\text{inh}} \cdot t_w \cdot r_w \quad (5)$$

and for stomach the annual effective dose is given by,

$$\delta_{\text{stomach}}\,(\mu Sv^{-1}) = \delta_{\text{ing}} \cdot t_w \cdot r_w \quad (6)$$

where δ_{inh} is the annual inhalation dose (for lungs), and δ_{ing} is the annual ingestion dose (for stomach) (in *Sv*), t_w is the tissue weighting factor (0.12 for lung and stomach), and r_w is the radiation weighting factor (20 for alpha particles, 1.0 for beta particle and 1.0 for gamma ray (Vajuhudeen and Morgan, 2020).

2.5.2 Lung cancer cases per million per year

The potential number of lung cancer cases per million individuals per year is estimated as (Pervin et al., 2022),

$$\lambda_l = \delta_{\text{inh}} \cdot r_f \quad (7)$$

where δ_{inh} is the annual effective dose in $\mu Sv/y$, and $r_f = 18 \times 10^{-3}\ \mu Sv^{-1} \cdot y$ is the risk factor for lung cancer induction.

2.5.3 Excess lifetime cancer risk

The excess lifetime cancer risk, $\mathcal{E}_r$ is estimated as (Sherafat et al., 2019),

$$\mathcal{E}_r = \delta_t \cdot \tau \cdot r_f \quad (8)$$

where τ is the average duration of life (assumed to be 70 *years*), and r_f is the fatal cancer risk per Sievert ($5.5 \times 10^{-2}\ Sv^{-1}$) (ICRP, 2007).

3. Results

The lab measurement of ^{222}Rn concentrations in the water samples was performed using a Tri-Carb-LSA 1000 liquid scintillation counter (Table 2). Calibration was conducted with IAEA ^{226}Ra standard solutions. Background, calibration, and sample solutions were analyzed within the same spectral range over a 60-min counting period.

Table 3 shows the concentration of ^{222}Rn in drinking water samples from the 28 locations. The concentrations across the surveyed locations vary significantly, ranging from 2.84 *Bq/L* (WT10) to 12.35 *Bq/L* (WT22). This variation suggests heterogeneity in geological formations or underground aquifers influencing the radon content in the groundwater. The mean radon concentration across all the samples is 7.30 *Bq/L*, with three of the detections above the USEPA's maximum contaminant level of 11.1 Bq/L, namely WT22 (12.35 *Bq/L*), WT23 (11.72 *Bq/L*), and WT04 (11.33 *Bq/L*). Although only a few exceed the limit, a considerable number fall within the range of moderate concern (6–10 Bq/L). This suggests a potential chronic exposure risk, particularly for populations relying solely on these groundwater sources for daily consumption. While most concentrations are below the WHO's recommended action level of 100 Bq/L, long-term ingestion of water with levels between 7–12 Bq/L could still contribute meaningfully to internal radiation dose. Chronic exposure could increase the risk of stomach or gastrointestinal cancers.

Mitigation techniques such as water aeration before use or switching to alternative water sources is recommended in high-risk areas. Public awareness campaigns should also be launched to educate communities on the risks of radon ingestion and methods to reduce exposure. These steps are vital to safeguarding public health in Borno State and enhancing environmental radiation protection measures.

Table 2: Specifications of Tri-Carb LSA 1000 liquid scintillation counter used in this study

Parameter	Specification
Model	Tri-Carb LSA 1000 (PerkinElmer, USA)
Detector Type	Liquid Scintillation Counter (alpha/beta discrimination with PSA)
Sample Capacity	20 *mL* low-diffusion glass scintillation vials
Energy Range	0 – 2000 *keV*
Counting Efficiency	~90–95% for ^{222}Rn in selected energy windows (determined by SQP[E] calibration)
Quench Correction	External standard method using ^{133}Ba
Reference Materials for Calibration	NIST-traceable ^{226}Ra solution (radon equilibrium ingrowth); ^{133}Ba external gamma source
Software	Tri-Carb Data Management System (TDMS)/Quanta Smart for spectral acquisition

Table 3: The mean concentration of ^{222}Rn in drinking water samples of five LGAs of Borno State

Sample ID	Site	LGA	Latitude	Longitude	Temp (°C)	Humidity (%)	C_{Rn} (BqL^{-1})
WT01	Goniri Njimtilo	Konduga	12.432778	13.034444	33	11	9.92
WT02	Kalari Njimtilo		12.405000	13.032222	34	11	10.26
WT03	Jewu/ Lamboa Njimtilo		12.405000	13.669722	36	10	3.12
WT04	Usmanti		11.854167	13.218889	34	13	11.33
WT05	Mala Kaleri		11.850556	13.219167	36	12	4.28
WT06	Moramti	Maiduguri	12.421667	13.089722	38	08	7.67
WT07	77 Housing Estate		12.405000	12.118889	38	10	9.32
WT08	Ngomari Bus stop		12.377222	13.156389	38	08	7.62
WT09	Gwange Layin Juma'a		11.083611	13.163611	26	20	6.56
WT10	Gwange Layin Gida Kifi		11.833056	13.017222	29	17	2.84
WT11	Gwange Layin Mai Dara		11.829722	13.165011	32	16	4.84
WT12	Gwange Barrack		11.825278	13.162222	32	14	5.69
WT13	Gwange IV		11.826944	13.016944	33	13	7.41
WT14	Gwange Layin Gidan Zana		11.809167	13.183611	35	12	5.60
WT15	Gwange Kasuwan Dare		11.833056	13.017222	35	11	8.30
WT16	Gwange Layin Makaranta		11.085000	13.024722	29	20	3.15
WT17	Gwange Mukaddam Usman Street		11.829167	13.025833	29	18	6.72
WT18	Gwange Layin City Robber		11.829167	13.027222	32	14	5.44
WT19	Mala Kyariri	Mafa	11.853333	13.218611	37	10	4.30
WT20	Mala Kyariri I		11.850278	13.210556	37	12	7.80
WT21	Kaleri Layin Church		11.830833	13.194167	31	18	7.39
WT22	Goni Kachallari	Jere	11.856389	13.212778	37	10	12.35
WT23	UMTH I		11.827500	13.032222	31	18	11.72
WT24	UMTH II		11.827222	13.026667	29	18	8.52
WT25	London Ciki		11.084444	13.028056	34	16	8.41
WT26	Kajari	Magumeri	12.113611	12.828056	35	09	5.18
WT27	Tashan Mata		12.113611	12.832778	34	10	8.37
WT28	Opp. Vocational Center		12.110833	12.828333	34	10	10.81
Min Value							2.84
Max Value							12.35
Mean Value							7.32
USEPA, 1991							11.1

For comparison, ^{222}Rn concentrations in groundwater elsewhere is given in Table 4.

Table 5 presents the total annual effective doses (δ_{total}) of ^{222}Rn for males and females across various age groups in five localities. Across all the locations, the total effective doses vary widely, with values ranging from as low as 2.01 $\mu Sv\ y^{-1}$ in Maiduguri to a maximum of 69.49 µSv y^{-1} in Jere for males. For females, doses

range from 2.21 $\mu Sv\ y^{-1}$ (Konduga) to 64.52 $\mu Sv\ y^{-1}$ (Jere). Thus, Jere recorded the highest average doses for both sexes, with female mean values peaking at 53.55 $\mu Sv\ y^{-1}$ and male values at 57.68 $\mu Sv\ y^{-1}$.

Table 4: ^{222}Rn concentrations in groundwater from literatures, for comparison with the current study results

Region / Study Area	^{222}Rn (Bq/L)	Reference
Kaya, Burkina Faso	-90	Elola et al., 2023
Wa, Ghana	~30-85	Amarh et al., 2023
Edu, Kwara-Nigeria	24.16± 4.21	Ajibola et al., 2021
Bahabad, Iran	13.8 Â± 3.5	Darabi et al., 2020
Shanono, Kano-Nigeria	3.18-49.93	Bello et al., 2020
Sulaymania, Iraq	35-95	Salih et al., 2019
Ijero, Ekiti-Nigeria	0.168-78.5	Akinnagbe et al., 2018
South Baghdad Suburbs, Iraq	45-110	Amin et al., 2018
Idah, Kogi-Nigeria	13.45± 1.00	Aruwa et al., 2017
Southwestern Nigeria	-82	Olise et al., 2016
Kerman, Iran	15.62	Asadi et al., 2016
Baghdad, Iraq	20-75	Amin et al., 2015
Zaria, Kaduna-Nigeria	7.41± 2.04	Garba et al., 2012
Cyprus	0.3-20.0	Nikolopoulos & Louizi, 2008
Greece	0.8-24.0	Nikolopoulos & Louizi, 2008
Brazil	0.95-36	Marques et al., 2004
Busan, South Korea	0-300.0	Cho et al., 2004
Cyprus	0.1-5 (mean 1.4)	Sarrou & Pashalidis, 2003

Table 5: The calculated total annual effective dose of ^{222}Rn from the water samples

Location	δ_{total} $(\mu Sv\ y^{-1})$															
	Female (*i*)									Male (*i*)						
	1	2	3	4	5	6	7	8	9	1	2	3	4	5	6	7
	7.03	20.88	24.34	26.11	32.25	35.33	36.81	40.9	51.81	27.5	20.88	24.34	26.11	36.86	50.69	55.8
	7.28	21.61	25.20	27.03	33.39	36.57	38.11	42.34	53.63	28.47	21.61	25.2	27.03	38.16	52.47	57.77
Konduga	2.21	6.57	7.66	8.21	10.15	11.11	11.58	12.87	16.30	8.65	6.57	7.66	8.21	11.60	15.94	17.55
	8.03	23.85	27.81	29.83	36.85	40.36	42.06	46.73	59.19	31.42	23.85	27.81	29.83	42.12	57.91	63.76
	3.04	9.01	10.51	11.27	13.93	15.25	15.89	17.66	22.37	11.87	9.01	10.51	11.27	15.92	21.88	24.09
	5.43	16.14	18.82	20.19	24.93	27.31	28.46	31.62	40.05	21.26	16.14	18.82	20.19	28.50	39.18	43.14
	6.61	19.63	22.89	24.55	30.33	33.21	34.61	38.46	48.71	25.86	19.63	22.89	24.55	34.66	47.65	52.46
	5.40	16.04	18.71	20.07	24.79	27.15	28.29	31.43	39.81	21.13	16.04	18.71	20.07	28.33	38.95	42.88
	4.65	13.80	16.09	17.26	21.33	23.36	24.34	27.04	34.25	18.18	13.80	16.09	17.26	24.37	33.51	36.89
	2.01	5.98	6.97	7.48	9.24	10.12	10.54	11.72	14.84	7.88	5.98	6.97	7.48	10.56	14.52	15.98
	3.43	10.19	11.88	12.74	15.74	17.24	17.97	19.96	25.29	13.42	10.19	11.88	12.74	17.99	24.74	27.23
Maiduguri	4.03	11.97	13.96	14.98	18.50	20.26	21.11	23.46	29.71	15.77	11.97	13.96	14.98	21.14	29.07	32.01
	5.26	15.61	18.20	19.52	24.12	26.41	27.53	30.58	38.74	20.56	15.61	18.20	19.52	27.56	37.90	41.72
	3.97	11.78	13.74	14.74	18.20	19.94	20.78	23.08	29.24	15.52	11.78	13.74	14.74	20.81	28.61	31.49
	5.88	17.48	20.38	21.86	27.00	29.57	30.82	34.24	43.37	23.02	17.48	20.38	21.86	30.86	42.43	46.71
	2.23	6.63	7.73	8.29	10.24	11.21	11.68	12.98	16.44	8.73	6.63	7.73	8.29	11.70	16.09	17.71
	4.76	14.14	16.49	17.69	21.85	23.93	24.93	27.70	35.09	18.63	14.14	16.49	17.69	24.97	34.33	37.80
	3.86	11.45	13.35	14.32	17.69	19.38	20.19	22.44	28.42	15.09	11.45	13.35	14.32	20.22	27.80	30.61
	3.05	9.05	10.55	11.32	13.98	15.31	15.96	17.73	22.46	11.92	9.05	10.55	11.32	15.98	21.97	24.19
Mafa	5.53	16.42	19.14	20.53	25.37	27.78	28.95	32.17	40.74	21.63	16.42	19.14	20.53	28.99	39.86	43.88
	5.24	15.55	18.13	19.45	24.03	26.31	27.42	30.47	38.59	20.48	15.55	18.13	19.45	27.46	37.76	41.57
	8.75	26.00	30.31	32.51	40.17	43.99	45.84	50.93	64.52	34.24	26	30.31	32.51	45.9	63.12	69.49
Jere	8.31	24.68	28.77	30.86	38.12	41.75	43.51	48.34	61.23	32.50	24.68	28.77	30.86	43.57	59.91	65.95
	6.04	17.94	20.92	22.44	27.72	30.35	31.63	35.15	44.52	23.63	17.94	20.92	22.44	31.67	43.55	47.95
	5.96	17.71	20.64	22.14	27.35	29.96	31.22	34.69	43.93	23.32	17.71	20.64	22.14	31.26	42.98	47.32
	3.67	10.9	12.71	13.63	16.84	18.45	19.22	21.36	27.05	14.36	10.9	12.71	13.63	19.25	26.47	29.14
Magumeri	5.94	17.63	20.56	22.05	27.24	29.83	31.09	34.54	43.75	23.22	17.63	20.56	22.05	31.13	42.8	47.12
	7.66	22.75	26.53	28.45	35.15	38.50	40.12	44.57	56.46	29.97	22.75	26.53	28.45	40.17	55.23	60.81

In contrast, Maiduguri exhibited the lowest average doses, with female and male mean values of 32.61 $\mu Sv\ y^{-1}$ and 35.13 $\mu Sv\ y^{-1}$, respectively. Although none of the total annual effective doses exceeded the World Health Organization recommended reference dose level of 100 $\mu Sv\ y^{-1}$, certain individual values (such as, Jere (WT22), male: 69.49 μSvy^{-1}) are recorded concerning thresholds. The findings underscore the necessity for continued monitoring and the implementation of mitigation strategies, especially in Jere and Magumeri.

Age, location, and physiological state all raised the annual effective doses from ^{222}Rn ingestion (mean ± uncertainty), as shown in Table 6. The lowest exposures were found in infants (0–6 months; 4.43 ± 0.22 $\mu Sv\ y^{-1}$ in Maiduguri; 7.27 ± 0.36 $\mu Sv\ y^{-1}$ in Jere); however, adolescents (14–18 years: 36.51 ± 1.83 $\mu Sv\ y^{-1}$ in Jere females; 41.50 ± 2.08 $\mu Sv\ y^{-1}$ in Magumeri males) and adults (>19 years: up to 57.68 ± 2.88 $\mu Sv\ y^{-1}$ in Jere males) had the highest exposures. The highest exposures were observed during pregnancy and lactation, peaking at 53.55 ± 2.68 $\mu Sv\ y^{-1}$ in Jere and 42.42 ± 2.12 $\mu Sv\ y^{-1}$ in Magumeri. Thus, Jere and Magumeri displayed greater values than Maiduguri and Mafa, and males consistently out dosed females. The higher doses in susceptible groups underscore the need for targeted monitoring and mitigation in high-risk areas, even if all values were below the WHO ingestion limit. The dose distribution was strongly impacted by age group differences, with older groups (adults and adolescents) exhibiting higher ingestion doses as a result of increased body mass and water intake, emphasizing the importance of age- and sex-specific assessment in radiological health studies. Compared to substantially lower levels in minors (e.g., 16.05 ± 0.80 $\mu Sv\ y^{-1}$ for females and 13.14 ± 0.66 $\mu Sv\ y^{-1}$ for males in Maiduguri), the yearly mean doses in Jere were 53.55 ± 2.68 $\mu Sv\ y^{-1}$ for adult females and 57.68 ± 2.88 $\mu Sv\ y^{-1}$ for adult males. However, since children's developing organs, higher cell turnover, and longer lifespans for latent effects to manifest make them more radiosensitive, these higher absolute levels in adults may not necessarily translate into increased radiological danger. This suggests that even very low doses in children may have biological effects that are proportionately higher, highlighting the necessity of sex- and age-specific evaluations in radiological health investigations.

The organ-specific annual effective doses for both lungs and stomach (Table 7) show that alpha particles contribute disproportionately higher doses compared to beta particles, primarily due to their significantly higher radiation weighting factor (r_w = 20).

Table 6: Mean annual effective dose from ^{222}Rn ingestion ($\mu Sv\ y^{-1}$)

Location	Sex	1	2	3	4	5
Jere	Female	7.27 ± 0.36	21.58 ± 1.08	25.16 ± 1.26	26.99 ± 1.35	33.34 ± 1.67
	Male	28.42 ± 1.42	21.58 ± 1.08	25.16 ± 1.26	26.99 ± 1.35	38.10 ± 1.91
Konduga	Female	5.40 ± 0.27	16.05 ± 0.80	18.71 ± 0.94	20.07 ± 1.00	24.80 ± 1.24
	Male	21.14 ± 1.06	16.05 ± 0.80	18.71 ± 0.94	20.07 ± 1.00	28.34 ± 1.42
Mafa	Female	4.60 ± 0.23	13.67 ± 0.68	15.94 ± 0.80	17.10 ± 0.86	21.12 ± 1.06
	Male	18.01 ± 0.90	13.67 ± 0.68	15.94 ± 0.80	17.10 ± 0.86	24.14 ± 1.21
Magumeri	Female	5.76 ± 0.29	17.10 ± 0.86	19.93 ± 1.00	21.38 ± 1.07	26.41 ± 1.32
	Male	22.52 ± 1.13	17.10 ± 0.86	19.93 ± 1.00	21.38 ± 1.07	30.18 ± 1.51
Maiduguri	Female	4.43 ± 0.22	13.14 ± 0.66	15.32 ± 0.77	16.44 ± 0.82	20.30 ± 1.02
	Male	17.31 ± 0.87	13.14 ± 0.66	15.32 ± 0.77	16.44 ± 0.82	23.20 ± 1.16

Location	Sex	6	7	8	9
Jere	Female	36.51 ± 1.83	38.05 ± 1.90	42.28 ± 2.11	53.55 ± 2.68
	Male	52.39 ± 2.62	57.68 ± 2.88	–	–
Konduga	Female	27.16 ± 1.36	28.30 ± 1.42	31.44 ± 1.57	39.83 ± 1.99
	Male	38.96 ± 1.95	42.90 ± 2.15	–	–
Mafa	Female	23.14 ± 1.16	24.11 ± 1.21	26.79 ± 1.34	33.93 ± 1.70
	Male	33.20 ± 1.66	36.55 ± 1.83	–	–
Magumeri	Female	28.93 ± 1.45	30.14 ± 1.51	33.49 ± 1.67	42.42 ± 2.12
	Male	41.50 ± 2.08	45.69 ± 2.28	–	–
Maiduguri	Female	22.24 ± 1.11	23.17 ± 1.16	25.75 ± 1.29	32.61 ± 1.63
	Male	31.91 ± 1.60	35.13 ± 1.76	–	–

Table 7: Organ-specific annual effective Ddoses, excess lifetime cancer risk and estimated lung cancer

Sample Site	$\mathcal{E}_r(\%)$		Female($\mu Sv \cdot y^{-1}$)				Male($\mu Sv \cdot y^{-1}$)				λ_l (Per Million Population)	
			$\delta_{stomach}$		δ_{lung}		$\delta_{stomach}$		δ_{lung}			
	Female	Male	alpha	beta	Alpha	beta	alpha	beta	alpha	beta	Female	Male
WT01	0.014	0.021	70.36	3.52	17.99	0.90	109.27	5.46	24.65	1.23	134.93	819.54
WT02	0.015	0.022	72.83	3.64	18.62	0.93	113.12	5.66	25.52	1.28	139.68	848.38
WT03	0.004	0.007	22.13	1.11	5.66	0.28	34.37	1.72	7.76	0.39	42.45	257.8
WT04	0.016	0.025	80.38	4.02	20.56	1.03	124.84	6.24	28.17	1.41	154.16	936.33
WT05	0.006	0.009	30.38	1.52	7.77	0.39	47.18	2.36	10.64	0.53	58.26	353.83
WT06	0.011	0.017	54.39	2.72	13.91	0.70	84.47	4.22	19.06	0.95	104.31	633.54
WT07	0.013	0.020	66.15	3.31	16.91	0.85	102.74	5.14	23.18	1.16	126.86	770.52
WT08	0.011	0.017	54.07	2.70	13.83	0.69	83.97	4.20	18.95	0.95	103.69	629.79
WT09	0.009	0.014	46.52	2.33	11.89	0.59	72.25	3.61	16.30	0.82	89.21	541.84
WT10	0.004	0.006	20.15	1.01	5.15	0.26	31.30	1.56	7.06	0.35	38.65	234.73
WT11	0.007	0.010	34.34	1.72	8.78	0.44	53.33	2.67	12.03	0.60	65.85	399.97
WT12	0.008	0.012	40.35	2.02	10.32	0.52	62.67	3.13	14.14	0.71	77.39	470.04
WT13	0.011	0.016	52.61	2.63	13.45	0.67	81.70	4.09	18.43	0.92	100.89	612.78
WT14	0.008	0.012	39.71	1.99	10.15	0.51	61.67	3.08	13.91	0.70	76.15	462.54
WT15	0.012	0.018	58.90	2.94	15.06	0.75	91.47	4.57	20.64	1.03	112.95	686.03
WT16	0.004	0.007	22.33	1.12	5.71	0.29	34.68	1.73	7.82	0.39	42.83	260.11
WT17	0.010	0.015	47.66	2.38	12.19	0.61	74.01	3.70	16.70	0.83	91.40	555.11
WT18	0.008	0.012	38.60	1.93	9.87	0.49	59.94	3.00	13.52	0.68	74.02	449.57
WT19	0.006	0.009	30.50	1.53	7.80	0.39	47.37	2.37	10.69	0.53	58.49	355.27
WT20	0.011	0.017	55.33	2.77	14.15	0.71	85.93	4.30	19.39	0.97	106.11	644.50
WT21	0.011	0.016	52.41	2.62	13.40	0.67	81.40	4.07	18.37	0.92	100.51	610.48
WT22	0.018	0.027	87.61	4.38	22.40	1.12	136.07	6.80	30.70	1.54	168.03	1020.53
WT23	0.017	0.025	83.16	4.16	21.26	1.06	129.15	6.46	29.14	1.46	159.48	968.63
WT24	0.012	0.018	60.46	3.02	15.46	0.77	93.89	4.69	21.18	1.06	115.94	704.19
WT25	0.012	0.018	59.66	2.98	15.26	0.76	92.66	4.63	20.91	1.05	114.42	694.97
WT26	0.007	0.011	36.74	1.84	9.39	0.47	57.06	2.85	12.87	0.64	70.46	427.94
WT27	0.012	0.018	59.42	2.97	15.19	0.76	92.28	4.61	20.82	1.04	113.95	692.08
WT28	0.015	0.023	76.67	3.83	19.61	0.98	119.08	5.95	26.87	1.34	147.04	893.08

At WT22, the female lung dose from alpha particles is 30.70 μSv, while the beta contribution is only 1.54 μSv, indicating that alpha particles account for ~ 95% of the total lung dose. This pattern is consistent across all sample sites and for both organs, emphasizing the dominant role of alpha-emitting radionuclides such as uranium, radium, and polonium. Their prevalence in contaminated water sources highlights a critical risk pathway through inhalation and ingestion, underscoring the need for stringent monitoring and mitigation measures. The estimated lung cancer cases per a million people per year, λl, derived from annual lung doses and a risk factor of 18×10^{-6} $\mu Sv^{-1} \cdot year^{-1}$, exhibit substantial variation across the sampled sites, ranging from as low as 38.65 (female) and 234.73 (male) at WT10 to as high as 168.03 (female) and 1020.53 (male) at WT22.

Furthermore, the estimated lung cancer cases per a million people per year (λl) in high-risk areas such as WT22 (1020.53) exceed 1000 cases per million for males, which is a concerning statistic when compared to natural background radiation risks and baseline cancer incidence rates. The elevated λ_l values closely correspond with higher annual lung doses and Excess Lifetime Cancer Risk values observed at the same sites, particularly WT22, WT23 (968.63), and WT28 (893.08). High-risk locations such as WT22, WT23, WT04 (936.33), and WT28 exhibited consistently elevated values across all health risk metrics and warrant immediate regulatory and remedial intervention, likely due to their proximity to contaminated sources (flood-impacted areas) that facilitate ^{222}Rn mobilization. WT01 (819.54), WT02 (848.38), WT07 (770.52), and WT24 (704.19) to WT27 (692.08), show moderately elevated risks that

necessitate continued monitoring and potential mitigation. In contrast, Table 7 show that WT03 (257.8), WT10 (234.73), and WT16 (260.11) are low-risk zones with minimal contamination. This is suggesting relatively safe conditions for local water use.

The WHO recommends a reference dose level of 100 $\mu Sv/year$ (0.1 $mSv/year$) for radiation exposure from drinking water, beyond which remedial actions should be considered. Similarly, the ICRP advises that annual effective doses from ingestion of radionuclides in water should not exceed 0.1 $mSv/year$ for the general public. In this study, sample sites WT22, WT23, WT04, and WT28 show combined organ-specific annual effective doses (particularly for the lung and stomach) which exceed or approach the 100 $\mu Sv/year$ threshold, especially for females exposed to alpha radiation. The female lung dose from alpha particles alone at WT22 is 30.70 μSv, and when combined with stomach doses and beta contributions, the total exposure for some individuals could surpass the WHO's guideline level. Additionally, Excess Lifetime Cancer Risk, λ_l, values exceed the widely referenced threshold of 1×10^{-4} (0.01%), indicating that long-term exposure at high-risk sites could significantly increase the probability of developing radiation-induced cancers.

4. Discussion

The findings suggest that ^{222}Rn concentrations in groundwater in flood-affected districts of Maiduguri differ, and in Jere and Konduga, contamination levels over the USEPA's limit of 11.1 *Bq/L were detected*. These results are in agreement with observations that highlighted the larger dose contribution from alpha-emitting radionuclides because of their higher biological effectiveness and Linear Energy Transfer (LET) (Nunes et al., 2023; UNSCEAR, 2008). Moreover, they are in line with researches that relate high ^{222}Rn levels to hydrogeological and geological circumstances, especially in areas of granitic and fractured rock (Shivakumara et al., 2014; Cho et al., 2004). Hydrological events may improve the mobilization of naturally occurring radionuclides through enhanced soil permeability, water table oscillations, or the introduction of organic matter that accelerates radionuclide desorption, as suggested by the reported increase in radon levels following the flood. The necessity of radiological protection is highlighted by the high alpha particle contribution (>95%) to the total dose, particularly since studies from comparable environments in South Asia and Sub-Saharan Africa have confirmed that alpha-emitting radionuclides pose higher biological risks because of their high LET (Miederer et al., 2024).

The estimated organ-specific doses and the demographic differences in dose distribution are consistent with earlier research by Hakme et al. (2025) and UNSCEAR (2008), which emphasize that adults are more susceptible as they tend to consume more water. Additionally, the comparably larger dosages detected in males are consistent with behavioral and physiological trends, including metabolic activity (Nakamura et al., 2020). Concerns regarding chronic exposure hazards are heightened by the fact that the predicted extra lifetime cancer risks and probable lung cancer incidence in the most afflicted sites exceed the globally recognized threshold of 10^{-4} (Solomon et al., 2024; Berg et al., 2023). These findings emphasize the need to localize global radiological norms, especially in view of climate change-induced extreme weather events that may worsen groundwater pollution dynamics.

Notwithstanding its significant contributions, the study has several flaws. First, the temporal component of radon variability was not captured due to single-time sampling; thus, seasonal and post-event monitoring are suggested to be incorporated into future studies to better characterize fluctuation tendencies. Second, whereas the spatial distribution of the sampling sites is representative, some geological heterogeneities may not have been adequately taken into account. Geospatial modeling and regional study expansion could enhance risk prediction and guide stronger public health initiatives. All things considered, this study offers a vital starting point for further research on environmental radiological risk assessment in Nigeria's semi-arid and flood-prone areas.

Since the activity concentrations of ^{226}Ra, ^{232}Th, and ^{40}K radionuclides were not directly measured, radium equivalent activity (Ra_{eq}), a commonly used hazard index for evaluating the combined radiological effects of these radionuclides in environmental samples (UNSCEAR, 2008), was not computed in this study. Ra_{eq} may have offered an extra confirmation of the

radon concentrations that were detected, because ^{226}Ra is the parent radionuclide of ^{222}Rn. However, the current findings provide useful baseline data on radon activity in the research region. To determine Ra_{eq} and create a more thorough comparison with worldwide safety standards, future research should include gamma spectrometric detection of ^{226}Ra, ^{232}Th, and ^{40}K in soil, sediment, or water samples.

5. Conclusion

This study investigated radon-222 concentrations in groundwater across 28 sites in five flood-affected localities in Borno, using a Tri-Carb-LSA 1000 Liquid Scintillation Counter. The results revealed spatial variations, with some sites (particularly in Jere and Konduga) exceeding the USEPA maximum contaminant level. The computed total annual effective doses ranged from 6.57-69.49 *μSv/y* for males and 2.01-64.52 *μSv/y* for females. Over 95% of the dose contributions were attributed to alpha particle emissions due to its high Linear Energy Transfer and significant carcinogenic potential. Excess lifetime cancer risk, λ_l and projected lung cancer incidence were found to exceed internationally acceptable thresholds in high-risk sites such as WT22, WT23, WT04, and WT28. These elevated values signal serious public health implications and the need for immediate environmental and regulatory intervention.

The study offers essential baseline data linking flood events to radon mobilization in groundwater, laying foundation for future research and public health preparedness in flood-prone areas. The correlation between hydrological disturbances and radionuclide transport reinforces the need for integrated water quality management and targeted risk communication strategies in affected communities. Age, sex, location, and physiological state all affected the annual effective doses from radon-222 consumption; the largest exposures were found in adults and adolescents, especially during pregnancy and lactation. Males typically outperformed females, while Jere and Magumeri continuously displayed higher values than Maiduguri and Mafa. The higher exposures in susceptible groups and children's higher radiosensitivity suggest that even lower doses may present proportionately higher risks, even though all measured doses were below the WHO ingestion limit. These results highlight the necessity of tailored mitigation initiatives and ongoing, age- and sex-specific monitoring in high-risk areas.

Based on the findings, it is recommended to establish routine groundwater monitoring programs, especially in high-risk and flood-prone zones. Public education campaigns should be initiated to raise awareness about radon exposure and promote behavioral and technological mitigation strategies. Regulatory frameworks must mandate radon testing in drinking water systems, particularly post-flooding, and encourage the adoption of cost-effective mitigation technologies such as aeration and activated carbon filtration. Furthermore, flood risk management plans should incorporate groundwater contamination risks, while investments in local capacity building for radon assessment and control should be prioritized to safeguard public health in vulnerable regions.

Acknowledgements: The authors gratefully acknowledge the Tertiary Education Trust Fund (TETFund), Nigeria, for financial support through an Institutional-Based Research (IBR) Grant. We also thank the University of Maiduguri's Department of Physics for providing lab space and technical support, especially from Muhammad A. Muhammad. Lastly, we express our gratitude to the leaders of the local community for their collaboration throughout the fieldwork.

Reference

Ajibola, T. B., Orosun, M. M., Lawal, W. A., Akinyose, F. C., & Salawu, N. B. (2021). Assessment of annual effective dose associated with radon in drinking water from gold and bismuth mining area of Edu, Kwara, North-central Nigeria. *Pollution*, 7(1), 231–240.

Akinnagbe, D. M., Orosun, M. M., Orosun, R. O., Osanyinlusi, O., Yusuk, K. A., Akinyose, F. C., Olaniyan, T. A., & Ige, S. O. (2018). Assessment of radon concentration of ground water in Ijero-Ekiti. *Manila Journal of Science*, 11, 32–41.

Ali, N., Khan, E. U., Akhter, P., Khan, F., & Waheed, A. (2010). Estimation of mean annual effective dose through radon concentration in the water and indoor air of Islamabad and Murree. *Radiation Protection Dosimetry*, 141(2), 183–191.

Amarh, F. A., Ashong, G. W., Agorku, E. S., Voegborlo, R. B., & Atongo, G. A. (2023). Health risk assessment of some selected heavy metals in infant food sold in Wa, Ghana. *Heliyon*, 9, e16225.

Amin, S. A., Alalgawi, S. D., & Hashim, H. M. (2015). Indoor radon concentrations and effective dose estimation in Al-Karkh side of Baghdad dwellings. *Iranian Journal of Science and Technology, Transactions A: Science*, 39(4), 491–495.

Amin, S. A., Al-Khateeb, M. A. W., & Al Shammari, T. A. (2018). Assessment of radon concentrations in the soil of South Baghdad suburbs. *Ibn Al-Haitham Journal for Pure and Applied Sciences*, 31(2).

Amin, S. A., Al-Obiady, A. H., & Alwan, A. (2017). Radon level measurements in soil and sediments at oil field area and its impact on the environment. *Engineering and Technology Journal*, 35(B1).

Aruwa, A. A., Kassimu, A. P., Gyuk, B., Ahmadu, J., & Aniegbu, J. (2017). Studies on radon concentration in underground water of Idah, Nigeria. *International Journal of Research - Granthaalayah*, 5(9), 266–274.

Asadi, M. A. A., Rahimi, M., & Jabbari, K. L. (2016). The effect of geological structure on radon concentration dissolved in groundwater in nearby Anar fault based on a statistical analysis. J Radioanalytical and Nuclear Chemistry, 308, 801–807.

Bello, M. S., Umar, I., & Yusuf, S. D. (2025). Assessment of radon-222 concentration in ground water from Dogarawa, Zaria, Kaduna State, Nigeria. *Dutse Journal of Pure and Applied Sciences*, 11(1b), 273–281.

Bello, S., Nasiru, R., Garba, N. N., & Adeyemo, D. J. (2020). Annual effective dose associated with radon, gross alpha and gross beta radioactivity in drinking water from gold mining areas of Shanono and Bagwai, Kano State, Nigeria. *Microchemical Journal*, 154, 104551

Berg, C. D., Schiller, J. H., Boffetta, P., Cai, J., Connolly, C., Kerpel-Fronius, A., Borondy Kitts, A., Lam, D. C. L., Mohan, A., Myers, R., Suri, T., Tammemagi, M. C., Yang, D., & Lam, S. (2023). Air pollution and lung cancer: A review by International Association for the Study of Lung Cancer Early Detection and Screening Committee. *J. Thoracic Oncology*, 18(10), 1277–1289.

Binesh, A., Mohammadi, S., Mowavi, A. A., & Parvaresh, P. (2010). Evaluation of the radiation dose from radon ingestion and inhalation in drinking water. *International Journal of Water Resources and Environmental Engineering*, 2(7), 174–178.

Celen, Y. Y., Gunay, O., Oncu, S., & Narin, B. (2023). Measurement of soil radon concentration in Balikesir and examination of its effects on health. *Journal of Radiation Research and Applied Sciences*, 16, 100718.

Cho, J. S., Ahn, J. K., Kim, H.-C., & Lee, D. W. (2004). Radon concentrations in groundwater in Busan measured with a liquid scintillation counter method. *Journal of Environmental Radioactivity*, 75(1), 105–112.

Darabi, F. Z., Rahimi, M., Malakootian, M., & Javid, N. (2020). Studying radon concentration in drinking water resources in Zarand city (Iran) and its villages. *Journal of Radio Analytical and Nuclear Chemistry*.

Darby, S., Hill, D., Auvinen, A., Barros-Dios, J. M., Baysson, H., Bochicchio, F., ... & Ruano-Ravina, A. (2005). Radon in homes and risk of lung cancer: collaborative analysis of individual data from 13 European case-control studies. *BMJ*, 330(7485), 223.

Deveci, F. O., & Oncel, M. S. (2023). Assessment of radiological hazard due to natural radioactivity in soils from agricultural areas of Turkey. *Chemosphere*, 311, 136991.

Duggal, V., Rani, A., & Mehra, R. (2012). In situ measurements of radon levels in groundwater in Northern Rajasthan, India. *Advances in Applied Science Research*, 3(6), 3825–3830.

Eikenberg, J. (2002). Radium isotope systematics in nature: Applications in geochronology and hydrogeochemistry [Habilitation thesis, Swiss Federal Institute of Technology (ETH) Zürich]. ETH Zurich Research Collection. https://doi.org/10.3929/ethz-a-004444917

El-Arabya, E. H., Soliman, H. A., & Abo-Elmagd, M. (2019). Measurement of radon levels in water and the associated health hazards in Jazan, Saudi Arabia. *Journal of Radiation Research and Applied Sciences*, 12(1), 31–36.

Elola, W. A., Bambara, T. L., Doumounia, A., Kohio, N., Ouédraogo, S., & Zougmore, F. (2023). Assessment of radon concentrations inside residential buildings and estimation of the dose in the city of Kaya, Burkina Faso. *Open Journal of Applied Sciences*, 13, 1066–1078.

Fan, Z., Xie, R., Cai, X., Hu, T., Luo, Y., Qin, F., Qiu, S., Tan, Y., & Shan, J. (2023). Determining the calibration factor of Rn-220 by low-pressure scintillation cell. *Metrologia*, 60(4), 045009.

Garba, N. N., Rabi'u, N., & Dewu, B. B. M. (2012). Preliminary studies on ^{222}Rn concentration in ground water from Zaria, Nigeria. *Journal of Physical Sciences*, 23(1), 57–64.

Goni, I. B., Sheriff, B. M., Kolo, A. M., & Ibrahim, M. B. (2019). Assessment of nitrate concentrations in the shallow groundwater aquifer of Maiduguri and environs, Northeastern Nigeria. *Scientific African*, 6, e00089.

Hakme, M., Francis, Z., Rizk, C., & Fares, G. (2025). Assessment of organ dose for adult undergoing CT examinations: Comparison of three software applications using Monte Carlo simulation. *Applied Radiation and Isotopes*, 220, 111740.

Howard, G., Bartram, J., Williams, A., Overbo, A., Fuente, D., & Geere, J.-A. (2020). Domestic water quantity, service level and health (2nd ed.). World Health Organization. https://www.who.int/publications/i/item/9789240015241 (Adapted with permission from Institute of Medicine [US]. (2005). Dietary reference intakes for water, potassium, sodium, chloride, and sulfate. The National Academies Press.)

ICRP (1993). Protection against Radon-222 at Home and at Work. ICRP Publication 65. Ann. ICRP 23 (2).

ICRP. (2007). The 2007 Recommendations of the International Commission on Radiological Protection. ICRP Publication 103. Annals of the ICRP, 37(2–4). Oxford: Elsevier.

Janik, M. (2022). Radiation protection: Radon. *The Science of the Total Environment*, 814, 152732.

Kumar, M., Kumar, P., Agrawal, A., & Sahoo, B. K. (2022). Radon concentration measurement and effective dose assessment in drinking groundwater for the adult population in the surrounding area of a thermal power plant. *J Water and Health*, 20(3), 551.

Kwaghe, A.V., Ameh, J.A., Kudi, C.A., Ambali, A-G., Adesokan, H.K., Akinseye, V.O., Adelakun, O.D., Usman, J.G., & Cadmus, S.I. (2023). Prevalence and molecular characterization of Mycobacterium tuberculosis complex in cattle and humans, Maiduguri, Borno state, Nigeria: a cross-sectional study. *BMC Microbiology*, 23, 7.

Lorenzo-Gonzalez, M., Barros-Dios, J. M., & Ruano-Ravina, A. (2020). Synergistic effect of tobacco and radon on lung cancer: A systematic review. *Archivos de Bronconeumología* (English Edition), 56(1), 49–55.

Manzoor, F., Alaamer, A. S., & Tahir, S. N. (2008). Exposures to ^{222}Rn from consumption of underground municipal water supplies in Pakistan. *Radiation Protection Dosimetry*, 130(3), 392–396.

Marques, A.L., dos Santos, W., & Geraldo, L.P. (2004). Direct measurements of radon activity in water from various natural sources using nuclear track detectors. *Applied Radiation and Isotopes*, 60, 801–804,

Miederer, M., Benešová-Schäfer, M., Mamat, C., Kästner, D., Pretze, M., Michler, E., Brogsitter, C., Kotzerke, J., Kopka, K., Scheinberg, D. A., & McDevitt, M. R. (2024). Alpha-emitting radionuclides: Current status and future perspectives. *Pharmaceuticals*, 17(1), 76.

Mostafa, M., Olaoye, M. A., Ademola, A. K., Jegede, O. A., Saka, A. A., & Khalaf, H. (2022). Measurement of radon concentration in water within Ojo Axis of Lagos State, Nigeria. *Analytica*, 3, 325–334.

Nakale, J. A., Ayua, K. J., Uloko, F. O., & Haruna, B. S. (2023). Determination of radon concentration in selected groundwater sources in Obajana, Kogi State. Nigerian Journal of Physics, 32(1).

Nakamura, Y., H. Watanabe, A. Tanaka, M. Yasui, J. Nishihira, and N. Murayama. 2020. "Effect of Increased Daily Water Intake and Hydration on Health in Japanese Adults." *Nutrients*, 12 (4): 1191.

Nikolopoulos, D., & Louizi, A. (2008). Study of indoor radon and radon in drinking water in Greece and Cyprus: Implications to exposure and dose. *Radiation Measurements*, 43, 1305–1314.

Nunes LJR, Curado A, Lopes S.I. (2023). The Relationship between Radon and Geology: Sources, Transport and Indoor Accumulation. *Applied Sciences*. 13(13):7460.

Olise, F. S., Akinnagbe, D. M., & Olasogba, O. S. (2016). Radionuclides and radon levels in soil and groundwater from solid minerals-hosted area, South-western Nigeria. *Cogent Environmental Science*, 2, 1142344.

Pervin, S., Yeasmin, S., Khandaker, M. U., & Begum, A. (2022). Radon concentrations in indoor and outdoor environments of Atomic Energy Centre Dhaka, Bangladesh, and concomitant health hazards. *Frontiers in Nuclear Engineering*, 1, 901818.

Salih, N. F., Aswood, M. Sh., & Hamzawi, A. A. (2019). Effect of porosity on evaluation of radon concentration in soil samples collected from Sulaymania governorate, Iraq. IOP Conference Series: *J. Physics: Conference Series*, 1234(1), 012024.

Sarrou, I., & Pashalidis, I. (2003). Radon levels in Cyprus. *Journal of Environmental Radioactivity*, 68(3), 269–277.

Sextro, R. G. (1994). What is environmental equity?: The challenge of incorporating community values in risk assessment.

Sherafat S, Nemati Mansour S, Mosaferi M, Aminisani N, Yousefi Z, & Maleki S. (2019). First indoor radon mapping and assessment excess lifetime cancer risk in Iran. *MethodsX*. 6:2205-2216.

Shivakumara, B. C., Chandrashekara, M. S., Kavitha, E., & Paramesh, L. (2014). Studies on ^{226} Ra and ^{222}Rn concentration in drinking water of Mandya region, Karnataka State, India. *J. of Radiation Research and Applied Sciences*, 7(4), 491–498.

Solomon Demissie, Seblework Mekonen, Tadesse Awoke, Birhanu Teshome, & Bezatu Mengistie (2024). Examining carcinogenic and noncarcinogenic health risks related to arsenic exposure in Ethiopia: A longitudinal study. *Toxicology Reports*, 12, 100–110.

Sridhar, K. N., Seenappa, L., & Manjunatha, H. C. (2021). Decay chain of ^{222}Rn. *Proceedings of the DAE Symposium on Nuclear Physics*, 65, 405–406.

Umar, H. A., Mohammed, A. G., Yusuf, M. L., Garba, Y., & Lawal, I. (2024). Assessment of radiological health risk due to 226Ra, 232Th and 40K in soil samples around artisanal gold mining sites, Bukkuyum, Zamfara State, Nigeria. *Journal of Applied Science and Environmental Management*, 28(1), 15-22.

UNSCEAR. (1988). Sources and effects of ionizing radiation. Report to the General Assembly with annexes. United Nations.

UNSCEAR. (2008). Sources and effects of ionizing radiation. Report to the General Assembly with scientific annexes. UN.

USEPA. (1991). National Primary Drinking Water Regulations; Radionuclides; US Environmental Protection Agency Proposed Rule. Federal Register, 56, 33050-33127.

USEPA. (1991). National primary drinking water regulations; radionuclides: Proposed rule (Federal Register 40 Parts 141 and 142). U.S. Government Printing Office.

Vajuhudeen, Z., & Morgan, M. (2020, July 3). Radiation weighting factor. Radiopaedia.org. https://doi.org/10.53347/rID-79734 (Accessed August 12, 2025).

WHO. (2004). Guidelines for drinking-water quality (3rd ed., Vol. 1). World Health Organization.

WHO. (2011). Guidelines for drinking-water quality (4th ed.). World Health Organization Press. https://www.who.int/publications/i/item/9789241548151

Wilkening, M. (1990). The Behavior of Radon Daughters in the Indoor Environment. Indoor Air, 3(1), 1-14.